Distribution of terrace widths on a vicinal surface within the one-dimensional free-fermion model

B. Joós,* T. L. Einstein,† and N. C. Bartelt‡
Department of Physics, University of Maryland, College Park, Maryland 20742-4111
(Received 9 August 1990; revised manuscript received 21 November 1990)

For the terrace-step-kink model of a stepped surface, the distribution $P(L)$ of terrace widths L is calculated at low temperature by mapping the problem onto the one-dimensional free-fermion model. In this approximation, the only energetic interaction between steps is a hard-core repulsion. A skewed distribution with a parabolic rise and a Gaussian tail is found; the exact asymptotic forms are displayed. By plotting $\langle L \rangle P(L)$ vs $L/\langle L \rangle$, we obtain a "universal" curve nearly independent of the average terrace width $\langle L \rangle$. With use of this scaling property, analytic approximants are constructed and the role of correlations discussed. We present some results for steps with energetic interactions in two special cases.

I. INTRODUCTION

Surfaces cut close to high-symmetry directions (i.e., vicinal surfaces) tend to exhibit a regular array of meandering steps at temperatures below the roughening temperature of the high-symmetry facet direction.[1,2] With recent progress in scanning tunneling microscopy (STM), it has become possible to obtain quantitative information about such surfaces.[3] While the morphology of technically important systems might often be determined by kinetics,[4] it is also important to understand the *equilibrium* properties of such surfaces; this paper restricts itself to an analysis of such behavior. We assume that the steps do not cross each other, so that there are no overhangs; nor do steps terminate. We further assume that the dominant thermal excitation is the formation of kinks, leading to step meandering and thence entropic repulsion between the steps.[5,6] This approximation is expected to be valid until close to the roughening temperature of the terraces, when higher-energy excitations on the terraces (i.e., adatoms and voids) play an important role. These approximations embody the well-established terrace-step-kink (TSK) model.[7,8] An illustration of a possible configuration in such a model is shown in Fig. 1. Except at the end of the paper, we explicitly neglect energetic interactions between steps other than the hard-core exclusion preventing overhangs. Our principal motivation for considering noninteracting steps is not that we necessarily believe they correspond to reality for particular situations, but rather that we seek characteristic features of noninteracting models to which experimental data can be compared.

If there are no significant energetic interactions between steps, their structural properties can be described in terms of two characteristic lengths: The first is the average length d along the direction of step wandering, between close approaches of adjacent steps. This distance depends sensitively on the ratio of the kink energy to the temperature. By analyzing the thermal scaling properties of the structure factor in this direction, one should be able to extract this length and, ultimately, the kink energy from a high-resolution diffraction experiment, as described elsewhere.[6,9] An alternative approach using STM is to analyze the kink distribution.[10] In this paper we are concerned instead with the distribution $P(L)$ of *integer* terrace-width spacings L. These spacings are in the direction perpendicular to the average direction along which the step edge runs, i.e., in the direction of the projection onto a terrace of the normal to the vicinal surface. If energetic interactions do not introduce a competing length, properties in this direction—in particular $P(L)$, but also the structure factor[11]— depend almost exclusively on the second characteristic length, viz., the *average* spacing between steps, $\langle L \rangle$. This length is determined solely by the angle of misorientation ϕ. For

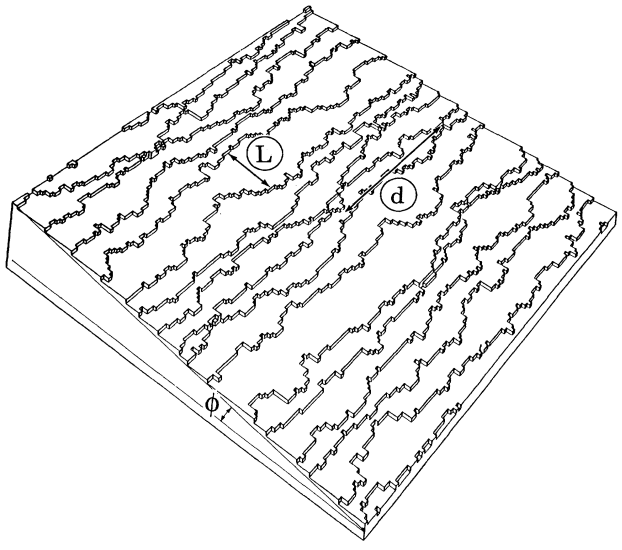

FIG. 1. Picture of a set of steps corresponding to a typical situation in the terrace-step-kink (TSK) model. The separation of steps at a given position along the step is shown as L. The average $\langle L \rangle$ is taken perpendicular to the average direction of the steps and parallel to them. The mean distance between step-step "collisions" is d.

single-height steps, $1/\langle L\rangle=\tan(\phi)$. Such properties should thus exhibit scant dependence on temperature.

As noted earlier, our work is motivated by recent STM studies to obtain terrace-width distributions. Extensive work has recently been done on Si(111) misoriented by 1.3° and 2.5° toward the $[2\bar{1}\,\bar{1}]$ direction[12] and on Si(001) miscut 1.3° toward [110],[10] and data on cleaved GaAs(110) is just becoming available.[13] At present, it is possible to make such rigorous measurements only at or near room temperature, at which the mobility of the sample is usually small. The observed distributions are thus characteristic of much higher, but ill-defined, temperatures at which the samples are annealed. When the kink density is low, we have shown[6] that the free-fermion model is an excellent approximation. In this model temperature does not influence $P(L)$; this fortunate feature thus facilitates comparison with experiment.

While it is not hard to generate numerical data for the TSK model using Monte Carlo simulations,[6] we would like to gain deeper insight into the form of the distribution. If only one type of step is allowed (usually single-layer steps), the problem is equivalent to that of the domain walls of a striped incommensurate two-dimensional phase.[7,14] As in this analogous problem, we can treat the steps as world lines of particles in a spinless one-dimensional (1D) fermion quantum field theory.[15] Essentially, we have a many-body quantum-mechanics problem. The direction along the steps is that of imaginary time, while that perpendicular to the steps is the 1D space along which the fermions are located at a given time. The meander excitations are related to the kinetic energy of the fermions or, more specifically, since this will be a discrete model, the hopping energy of the fermions. In the simplest situation the fermions are noninteracting, hence the appellation "free fermions."

The free-fermion model is a good approximation to the TSK model only at low temperatures. The temperature at which it breaks down depends on $\langle L\rangle$: Once the mean-square deviation at a possible kink site becomes comparable to $\langle L\rangle$, the approximation becomes poor. With Monte Carlo simulations,[6] we have verified for $\langle L\rangle=8$ that the terrace-width distribution obtained from free-fermion theory accurately describes the computed TSK distributions over the range of temperatures for which the TSK model itself is a viable approximation (to, for example, the solid-on-solid model, which admits terrace excitations[8]).

In this paper we adopt the following plan: In Sec. II we develop, within the formalism of the 1D free-fermion model, the correlation functions necessary to write $P(L)$. In Sec. III we show that the scaled form $\langle L\rangle P(L)$ plotted versus $L/\langle L\rangle$ has negligible dependence on $\langle L\rangle$ and describe the properties of this universal curve. In Sec. IV we use the scaling properties leading to the universal curve in order to set down a sequence of analytic approximants. The nth approximant takes into account correlations between $n+1$ fermions and accurately describes the distribution until $L/\langle L\rangle$ moderately exceeds $n/2$. We find that the third approximant accurately describes the physically important range of terrace widths and present an explicit expression. In Secs. V and VI we explore the behavior of the distribution at small and large values of $L/\langle L\rangle$, respectively. The asymptotic expression merges smoothly onto the third approximant, so that $\langle L\rangle P(L)$ can be well represented analytically for all $L/\langle L\rangle$. In the concluding section we indicate how interactions between steps modify our results. An appendix discusses some aspects of multiparticle correlations in this problem.

II. CORRELATION FUNCTIONS IN 1D FREE-FERMION THEORY

Our main interest is in the correlations of the particles. The problem is most easily considered a (discrete) ring with N sites. We begin with the well-known density-density correlation function or the two-particle correlation function:

$$G_0(L)=\langle 0|a_{n+L}^{\dagger}a_{n+L}a_n^{\dagger}a_n|0\rangle \ , \tag{1}$$

where $a_n^{\dagger}$ creates and a_n annihilates a fermion at site n. To obtain the correlations at equivalent positions along the steps, we seek the correlations at equal times for the two fermions. This correlation function is just the expectation value of the density operators with respect to the ground state of a 1D tight-binding model.[15–17] The calculation of $G_0(L)$ is then easy. Introducing the Fourier transforms in Eq. (1) yields[15,18]

$$G_0(L)=\frac{1}{N^2}\sum_{k,k',l,l'}\langle 0|a_k^{\dagger}a_{k'}a_l^{\dagger}a_{l'}e^{i(k-k')(n+L)}e^{i(l-l')n}|0\rangle \ . \tag{2}$$

Only two pairings contribute: (1) $k=k'$ and $l=l'$ and (2) $k=l'$ and $k'=l$. Hence,

$$G_0(L)=\frac{1}{N^2}\left[\sum_{k,l}\langle 0|\hat{n}_k\hat{n}_l|0\rangle-\sum_{k,k'}e^{i(k-k')L}\langle 0|\hat{n}_k\hat{n}_{k'}|0\rangle\right] . \tag{3}$$

The sums are evaluated for the ground state of the Fermi gas. Hence both particle-number operators have to be 1 for a term to contribute, and we have

$$G_0(L)=\frac{1}{N^2}\left[\left[\sum_{k=-k_F}^{k_F}1\right]^2-\left[\sum_{k=-k_F}^{k_F}e^{ikL}\right]\left[\sum_{k'=-k_F}^{k_F}e^{-ik'L}\right]\right] , \tag{4}$$

which equals

$$G_0(L)=Q^2-\frac{\sin^2(\pi QL)}{\pi^2L^2} \ , \tag{5}$$

where

$$Q=\frac{k_F}{\pi}=\frac{N_F}{N}=\frac{1}{\langle L\rangle} \ , \tag{6}$$

N_F being the total number of occupied states and Q the fraction of occupied states, while $\langle L \rangle$ is the *average* separation between steps, i.e., fermions. Note that $\langle L \rangle G_0(L)$ is a conditional probability (giving the probability of finding a fermion n sites away from a given fermion) and that $\langle L \rangle^2 G_0(L)$ is the scaled probability, which we could write

$$\frac{G_0(L)}{Q^2} = 1 - \left[\frac{\sin(\pi x)}{\pi x} \right]^2 , \tag{7}$$

where $x = QL = L/\langle L \rangle$. This scaled probability is independent of $\langle L \rangle$. It, however, does not exclude the possibility that there is an additional fermion or step between 0 and x, and this possibility becomes significant as x increases. To obtain the probability of having a terrace width of a given length, we must calculate the correlation between nearest fermions with *no* fermions in between; i.e., for $L \geq 2$ we have to calculate the multiparticle correlation function

$$G(L,Q) = \langle 0 | a_0^\dagger a_0 (1 - a_1^\dagger a_1) \cdots (1 - a_{L-1}^\dagger a_{L-1}) a_L^\dagger a_L | 0 \rangle . \tag{8}$$

Using particle-hole symmetry,

$$G(L,1-Q) = \langle 0 | (1 - a_0^\dagger a_0) a_1^\dagger a_1 \cdots a_{L-1}^\dagger a_{L-1} (1 - a_L^\dagger a_L) | 0 \rangle , \tag{9}$$

where $a_n^\dagger$ and a_n are now creation and annihilation operators for the holes. Expanding,

$$G(L) = \mathcal{G}(L+1) - 2\mathcal{G}(L) + \mathcal{G}(L-1) , \tag{10}$$

where

$$\mathcal{G}(L) = \langle 0 | a_0^\dagger a_0 a_1^\dagger a_1 \cdots a_{L-2}^\dagger a_{L-2} a_{L-1}^\dagger a_{L-1} | 0 \rangle \tag{11}$$

is the probability of having L particles (or L holes) occupying L consecutive sites. To evaluate $\mathcal{G}(L)$, one proceeds as previously. We transform to **k** space, perform the L^2 pairings, then integrate up the Fermi level to obtain a Toeplitz[19,20] determinant of order L. This is a determinant whose elements depend only on the difference between the row and column indices. The elements of $\mathcal{G}(L)$ are

$$a_{ij} = \begin{cases} \dfrac{\sin[\pi(1-Q)(i-j)]}{\pi(i-j)} & \text{if } i \neq j \\ 1-Q & \text{if } i = j . \end{cases} \tag{12}$$

The (conditional) probability of finding the first step L sites away from a given step can be written

$$P(L) = \frac{G(L,Q)}{Q} , \tag{13}$$

where we have introduced the additional variable which fully defines G_0. $P(L)$ is the terrace-width distribution we have been seeking.[6] Note that $P(L)$ is independent of temperature; i.e., the equal-time correlations are independent of the "mass" of the fermion.

III. PROPERTIES OF THE SCALED FUNCTION $\langle L \rangle P(L)$

Figure 2 shows the scaled distribution function $\langle L \rangle$ as a function of $x = L/\langle L \rangle$ for a wide range of values of $\langle L \rangle = 1/Q$. A rather surprising scaling is observed even for the smallest value of $\langle L \rangle = 2$. If we define

$$f(x) = \lim_{\langle L \rangle \to \infty} \langle L \rangle P(L) , \tag{14}$$

then the absolute error in approximating any point of $f(x)$ by a value of $\langle L \rangle P(L)$ is at most 0.002. For comparison, Fig. 2 also shows the large-$\langle L \rangle$ results for straight noninteracting steps, namely, $\exp(-x)$, and for a single particle confined to a 1D box of length $2\langle L \rangle$, namely, $\sin^2(\pi x/2)$. The latter result, obtained long ago by Gruber and Mullins[21] for a single step confined between two rigid walls separated by $2\langle L \rangle$, already captures most of the physics of the entropic repulsion,[5] which drastically reduces the probability of finding terraces with small L (and so also terraces with very large L).

From the numerical study the following observations can be made about $f(x)$.

(1) For small x the function increases quadratically, as in the Gruber-Mullins[21] model, but the coefficient is different: Instead of their $\pi^2 x^2/4$ behavior, we have

$$1 - \frac{\sin^2(\pi x)}{(\pi x)^2} \to \frac{\pi^2 x^2}{3} .$$

For a given small x, $\langle L \rangle P(L)$ is a (slowly) decreasing function of $\langle L \rangle$.

(2) The peak location is at $x_m = 0.8840$ and $f(x_m) = 0.9353$.

(3) The tail decays rapidly. The exact form is given in Sec. VI. Plots of $\ln[\langle L \rangle P(L)]$ versus x^2 are nearly

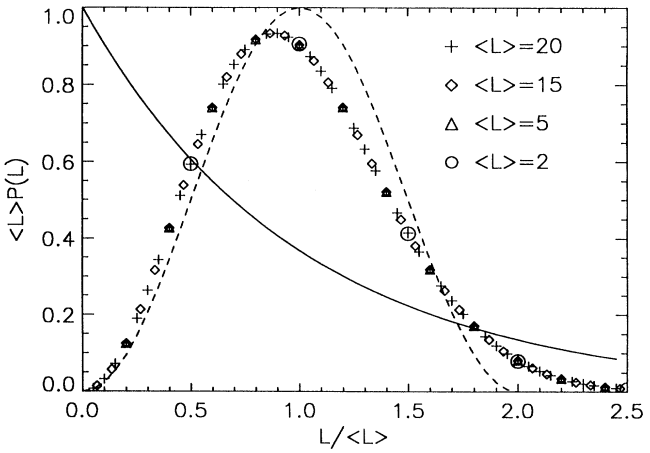

FIG. 2. Scaled terrace width distribution $\langle L \rangle P(L)$ generated with the formalism of Sec. II, for $\langle L \rangle = 2$, 5, 15, and 20. The scaling of this plot is dramatic. For comparison the solid curve shows the distribution for straight noninteracting steps (i.e., random placement of a fixed density of particles), while the dashed curve is for a single step meandering between fixed walls (i.e., a particle in a 1D box).

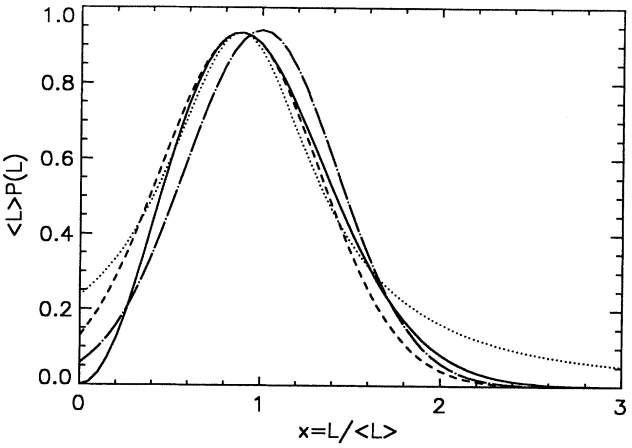

FIG. 3. Fit of the limiting "universal" terrace-width distribution $f(x)$ (solid curve) by a Lorentzian and two different Gaussians. The two parameters of the Lorentzian (dotted curve) were fit to the peak and the width at half maximum of $f(x)$. One Gaussian (short-dashed curve) was fit to the peak and its curvature. The other (long-dash–dotted curve) was determined from the mean and the variance of $f(x)$.

linear, with slope $\lesssim -1$. For equal (large) values of x, $\langle L\rangle P(L)$ is a (slowly) increasing function of $\langle L\rangle$: Increasing $\langle L\rangle$ is equivalent to decreasing the effective core size or the smallest relative distance of approach. This in effect makes large terrace widths slightly more likely.

(4) The mean of the distribution is 1 and its variance $\sigma^2=0.1800$. The skewness (with its definition) is given by

$$\gamma_1=\frac{\mu_3}{\sigma^3}=0.4972\ ,$$

where μ_3 is the third central moment of the distribution. Figure 3 shows that the distribution because of its non-negligible skewness cannot be fitted to any of the well-known distribution functions. The Lorentzian has been fitted to the half width at half maximum, while a Gaussian has been fitted to the peak region. The fit is much worse for the Gaussian if the mean and variance are matched rather than the peak region. Because of the unsatisfactory fit obtained with these two distributions and other functions, finding an analytical fit to the distribution is particularly worthwhile.

IV. ANALYTICAL APPROXIMANTS OF $\langle L\rangle P(L)$

The almost total lack of dependence of $\langle L\rangle P(L)$ on $\langle L\rangle$ will be used in this section to construct approximate forms for $f(x)$. $G(L,Q)$ is a function of both L and $Q=1/\langle L\rangle$. Since $QL=L/\langle L\rangle=x$, the scaled variable, we can write $G(L,Q)$ as $G(L,x)$, where rigorously $G(L,x)$ gives the appropriate correlation function or the scaled probability $G(L,x)Q^{-2}$ only for the set of discrete values $x=L/\langle L\rangle$. L is the number of lattice spacings between steps, and $\langle L\rangle$ is in units of lattice sites. For $L=1$, for instance,

$$G(1,Q)=Q^2-\frac{\sin^2(Q\pi)}{\pi^2} \tag{15}$$

or

$$\frac{G(1,x)}{Q^2}=\langle L\rangle^2 G(1,x)=1-\frac{\sin^2(\pi x)}{\pi^2 x^2} \tag{16}$$

is valid only for $x=1/l$, where l is an integer: one value of x for each possible value of $\langle L\rangle$, that value corresponding to fermions side by side in the discrete lattice.

Note that this function is the same as the scaled two-particle correlation function of Eq. (7). Because of the scaling observed in Fig. 2, we can use $G(1,x)Q^{-2}$ to approximate $f(x)$ over a continuous interval of x. We expect from the above to get good agreement for $x\le\frac{1}{2}$, $\frac{1}{2}$ being the largest allowed value in the above sequence. This is what is seen in Fig. 4. Actually, very good agreement is observed up to $x=0.65$ (error less than 1%). This interval corresponds to the region where the probability of having a second fermion in between 0 and x is small.

If we now consider $G(2,Q)$, which can be evaluated directly

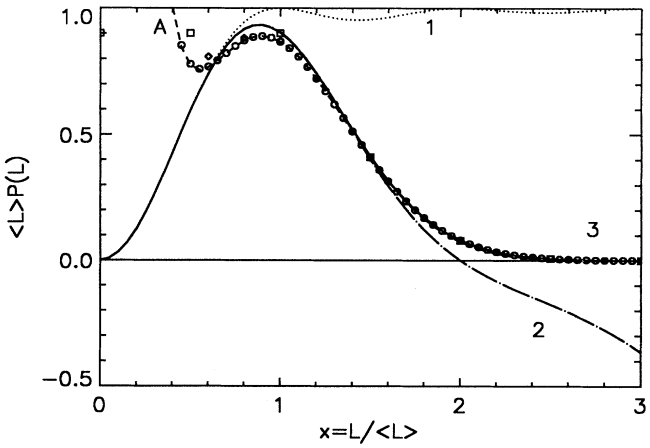

FIG. 4. Illustration of the viability and eventual breakdown of analytic approximants to the scaled distribution $f(x)$ (solid curve) of Eq. (14). As described in the text, the approximants have the form $Q^{-2}G(n,x)$ and take into account correlations of up to $n+1$ fermions. The dotted and long-dash–dotted curves correspond to $n=1$ and 2, respectively. The $n=3$ curve is indistinguishable from $f(x)$ over the range of this plot, but grows positive for larger x. These curves are analytical continuations of forms rigorously valid only for the discrete set of values $x=n/l$, where the l's are all positive integers starting with 2. We also show as (dashed) curve A the asymptotic scaled form given in Eq. (32). The circles show the full asymptotic $\mathcal{G}$ forms of Eq. (30), substituted into Eq. (10), for $\langle L\rangle=20$. Over most of the range of the plot, they are indistinguishable; for $2.0<x<2.6$, the former is slightly below $f(x)$. To assess the degree of breakdown at small $\langle L\rangle$, we show for $\langle L\rangle=2$ and 5 the results of Eq. (30) at $x=l/\langle L\rangle$ using squares and diamonds, respectively.

$$G(2,Q)=\langle 0|a_0^\dagger a_0(1-a_1^\dagger a_1)a_2^\dagger a_2|0\rangle \tag{17}$$

$$=\langle 0|a_0^\dagger a_0 a_2^\dagger a_2|0\rangle-\langle 0|a_0^\dagger a_0 a_1^\dagger a_1 a_2^\dagger a_2|0\rangle$$

$$=Q^2\left[1-\frac{\sin^2 2\pi Q)}{(2\pi Q)^2}\right]$$

$$-\begin{vmatrix} Q & \frac{\sin(Q\pi)}{\pi} & \frac{\sin(2Q\pi)}{2\pi} \\ \frac{\sin(Q\pi)}{\pi} & Q & \frac{\sin(Q\pi)}{\pi} \\ \frac{\sin(2Q\pi)}{2\pi} & \frac{\sin(Q\pi)}{\pi} & Q \end{vmatrix}, \tag{18}$$

or with $x=QL=2Q$ and defined

$$h(u)\equiv\frac{\sin(\pi u)}{\pi u}, \tag{19}$$

we can write

$$\frac{G(2,x)}{Q^2}=1-h^2(x)-\frac{x}{2}\left[1-2h^2\left[\frac{x}{2}\right]-h^2(x)+2h^2\left[\frac{x}{2}\right]h(x)\right]. \tag{20}$$

This function gives the scaled terrace-width distribution for

$$x=\frac{2}{\langle L\rangle}=1,\frac{2}{3},\frac{2}{4},\ldots,\frac{2}{l},$$

where l is an integer. An analytic extension of this function for a continuous set of values of x is then expected to give good estimates of $f(x)$ for x up to 1. As Fig. 4 shows, 1% agreement persists up to 1.4. This is the approximation which has been used to locate the peak position. Note that $G(2,2)Q^{-2}=0$, and as $x\to 2$,

$$G(2,x)Q^{-2}\to 1-\frac{x}{2}. \tag{21}$$

Similarly, we consider $G(3,Q)$. Using Eq. (10), we find

$$G(3,Q)=\mathcal{G}(4,1-Q)-2\mathcal{G}(3,1-Q)+\mathcal{G}(2,1-Q). \tag{22}$$

Evaluating the three determinants and replacing Q by $x=3Q$ yields the function

$$\frac{G(3,x)}{Q^2}=1-h^2(x)-\frac{2x}{3}\left\{1-\left[h^2\left[\frac{x}{3}\right]+h^2\left[\frac{2x}{3}\right]+h^2(x)\right]+2h\left[\frac{x}{3}\right]h\left[\frac{2x}{3}\right]h(x)\right\}$$
$$+\left[\frac{x}{3}\right]^2\left\{1-\left[3h^2\left[\frac{x}{3}\right]+2h^2\left[\frac{2x}{3}\right]+h^2(x)\right]+4h^2\left[\frac{x}{3}\right]h\left[\frac{2x}{3}\right]\right.$$
$$+4h\left[\frac{x}{3}\right]h\left[\frac{2x}{3}\right]h(x)+h^4\left[\frac{x}{3}\right]-2h^3\left[\frac{x}{3}\right]h(x)-2h^2\left[\frac{x}{3}\right]h^2\left[\frac{2x}{3}\right]$$
$$\left.+h^2\left[\frac{x}{3}\right]h^2(x)-2h\left[\frac{x}{3}\right]h\left[\frac{2x}{3}\right]h(x)+h^4\left[\frac{2x}{3}\right]\right\}. \tag{23}$$

The permitted values of x are

$$x=\frac{3}{\langle L\rangle}=\frac{3}{2},1,\frac{3}{4},\frac{3}{5},\ldots,\frac{3}{l},l \text{ integer}.$$

Hence we can expect in the analytical continuation to have very good agreement up to at least 1.5. Actually, $G(3,x)Q^{-2}$ is equal to zero at $x=3$ and approaches that value with zero slope as $(1-x/3)^2$. At $x=3$, $f(x)$ is less than 10^{-3}, and so we get a very good agreement over the whole relevant interval of values of x. This approximation underestimates $f(x)$ by less than 0.01 over [0,3]. For $x>3$, it starts rising. Its asymptotic behavior is $(1-x/3)^2$.

The next approximant $G(4,x)Q^{-2}$ goes to zero at $x=4$, with zero first and second derivative, behaving as $(1-x/4)^3$ in the neighborhood of $x=4$. In general, $G(n,x)Q^{-2}$ goes to zero at $x=n$ and its $(n-2)$ first derivatives are 0 at $x=n$. These results follow from the structure of the Toeplitz determinants. $G(n,x)Q^{-2}$ is a polynomial in $(1-Q)$ or $(1-x/n)$ (recall $nQ=x$) with leading term $(1-x/n)^{n-1}$. In the neighborhood of $x=n$, the coefficients to powers of $(1-x/n)^\gamma$ are of leading order $(x-n)^{n+1-\gamma}$. In short, about $x=n$,

$$\frac{G(n,x)}{Q^2}\simeq\left[1-\frac{x}{n}\right]^{n-1}. \tag{24}$$

This behavior gives a good indication of the kind of fit expected by the higher-order approximants. For practical purposes there is no need to consider any form higher than the $G(3,x)Q^{-2}$.

The way the various $G(n,x)Q^{-2}$ fit $f(x)$ measures the probability of having intermediate steps for different ranges of

x. $G(1,x)$ ignores the possibility that any step may occur in between 0 and x, and hence is equal to the density-density correlation function. It is a valid approximation until the probability of intervening steps becomes significant. $G(2,x)Q^{-2}$ allows the occupancy of a single intermediate step and therefore is valid until the probability of having two intermediate steps is appreciable, and so forth, for higher approximants.

V. EXPANSION OF $G(n,x)$ FOR SMALL x

To obtain an idea of the analytic form of the asymptotic function $f(x)$ at small x, we have attempted to expand $G(n,Q)$ in powers of Q or $x=Qn$. We do so by taking advantage of the structure of the Toeplitz determinant. As we know from Eq. (10),

$$G(n,Q)=\mathcal{G}(n+1,1-Q)-2\mathcal{G}(n,1-Q)+\mathcal{G}(n-1,1-Q)\ , \tag{25}$$

where we can write

$$\mathcal{G}(n,1-Q)=(1-Q)^n-(1-Q)^{n-2}\sum_{j=1}^{n-1}(n-j)\frac{\sin^2(\pi jQ)}{(\pi j)^2}+(1-Q)^{n-3}\left[\left[\sum 3\times 3 \text{ symmetric minors}\right]+\cdots\right]\ , \tag{26}$$

where the symmetric minors are all those with the same row and column indices as the 2×2 ones which yielded the preceding term. Similar procedures can yield the terms of any order. Making the usual replacement with x, the leading terms in $G(n,x)$ have the form

$$Q^{-2}G(n,x)=1-h^2(x)-\frac{x}{n}\left[(n-1)[1-h^2(x)]-\sum_{j=1}^{n-1}h^2\left[\frac{jx}{n}\right]+2h(x)\sum_{j=1}^{n-1}h\left[\frac{jx}{n}\right]h\left[x-\frac{jx}{n}\right]\right]$$
$$+\left[\frac{x}{n}\right]^2\left[\frac{1}{2!}(n-1)(n-2)-\sum h^2(\cdots)\cdots\right]\ . \tag{27}$$

The coefficient of the x term can be easily evaluated in the limit $n\to\infty$. In such a limit the sums can be replaced by integrals and we have

$$f(x)=1-h^2(x)-x\left[1-h^2(x)-\frac{2}{x}\int_0^x h(u)[h(u)-h(x)h(x-u)]du\right]+\cdots\ , \tag{28}$$

which can also be written as

$$f(x)=1-h^2(x)-x\left[1+h^2(x)-\frac{2}{\pi x}\mathrm{Si}(2\pi x)[1-h^2(x)]-\frac{2}{(\pi x)^2}h(2x)\mathrm{Cin}(2\pi x)\right]+\cdots\ , \tag{29}$$

where $\mathrm{Si}(u)$ and $\mathrm{Cin}(u)$ have the usual definitions

$$\mathrm{Si}(u)=\int_0^u\frac{\sin t}{t}dt,\quad \mathrm{Cin}(u)=\int_0^u\frac{1-\cos t}{t}dt\ .$$

The higher-order terms can be evaluated similarly.

VI. ASYMPTOTIC TAIL OF $\langle L\rangle P(L)$ OR $f(x)$

The above observation about the asymptotic behavior of $\langle L\rangle^2 G(L,x)$ brings us to the investigation of the asymptotic tail of $f(x)$. The numerical evidence as indicated in Sec. III shows that the leading dependence of the tail is $\exp(-ax^2)$, where $a\gtrsim 1$. For very large values of x, one begins to see small deviations from this simple form, but it can be difficult to assess how much is due to numerical difficulties.

The asymptotic limit of the distribution can be calculated rigorously using an extension by Widom[22] of the strong Szegö limit theorem, which gives the large-L limit of the Toeplitz determinant defining $\mathcal{G}(L)$ in Eq. (12). The elements of $\mathcal{G}(L)$ are the Fourier coefficients of a square-barrier distribution. The square barrier reflects the fact that we are dealing with the occupation function of a fermion gas at 0 K.[6] For such a distribution, the limit takes a relatively simple form:[22,23]

$$\mathcal{G}(L)\sim 2^{1/12}e^{3\zeta'(-1)}(L\cos\theta)^{-1/4}(\sin\theta)^{L^2}\ , \tag{30}$$

where $\theta=\pi(1-Q)/2$ and ζ' is the derivative of the Riemann ζ function.

If $\sin(\pi Q/2)$ can be approximated by $\pi Q/2$ and $\cos(\pi Q/2)$ by $1-\frac{1}{2}(\pi Q/2)^2$, the asymptotic form for $\mathcal{G}(L)$ becomes a function of only $x=QL$ and takes the simpler form

$$\mathcal{G}(x)\sim 2^{1/12}e^{3\zeta'(-1)}\left[\frac{\pi x}{2}\right]^{-1/4}e^{-\pi^2x^2/8}\ . \tag{31}$$

Thus, at large L, this Gaussian scaling expression must eventually break down, the larger Q the sooner.

The distribution function $G(L,Q)/Q^2$ as a function of x will have a similar asymptotic form since it is the second derivative with respect to x of the above distribution:

$$\frac{G(L,Q)}{Q^2} \sim 2^{1/12} e^{3\zeta'(-1)} \left[\frac{\pi}{2}\right]^2 \left[\frac{\pi x}{2}\right]^{7/4} e^{-\pi^2 x^2/8} \times \left[1-\frac{1}{2}\left[\frac{\pi x}{2}\right]^{-2}+\frac{5}{16}\left[\frac{\pi x}{2}\right]^{-4}\right] \tag{32}$$

As shown in Fig. 4, Eq. (32) gives remarkably good agreement with $f(x)$ above the peak region and even reproduces a peak, albeit with smaller magnitude, before diverging at small x. Over the entire plotted range, the scaled form is in excellent agreement with the exact asymptotic form of Eq. (30), for $Q=\frac{1}{20}$, inserted into Eq. (10). For $Q=\frac{1}{5}$ the agreement is fine; even for $Q=\frac{1}{2}$, it is very good until near the peak. For these larger values of Q, the asymptotic points are smaller than $f(x)$ by increasing amounts, but so are the curves for $G(L,Q)/Q^2$, as shown earlier in Fig. 2.

As a general statement, one can state that as discreteness becomes less important the tail behavior converges to a universal form fairly rapidly, although a nonnegligible Q dependence persists. The main result to be remembered is that for free noninteracting steps, the tail is Gaussian. This is reminiscent of the behavior of a set of self-avoiding walkers starting at adjacent sites along a line. The asymptotic distribution of these walkers also contains a Gaussian term.[24]

VII. CONCLUDING COMMENTS

This paper has assumed implicitly that the spatial and timelike directions of the steps lie along principal directions of a square lattice. Recent work[25] has shown how to generalize to arbitrary directions. We have checked[26] that the scaled distribution of terrace widths does not change significantly if the misorientation (tilt) is in an arbitrary azimuthal direction.

The analysis of this paper has assumed an (infinite) defect-free surface. Consequently, $P(L)$ is independent of temperature—temperature and kink energy enter the problem only as a dimensionless ratio determining the characteristic[5] distance d (cf. Fig. 1). Thus, defects might significantly influence $P(L)$, e.g., if they pin the step edges at intervals smaller than d. Since d increases rapidly with decreasing temperature,[5,6] this problem could be important for a (fully) equilibrated surface at low temperature.

In comparison to STM data for Si(111),[12] the above distribution, which assumes no energetic interactions, overestimates by a significant amount the probability of finding terraces with small widths (as well as, concomitantly, the probability of finding very wide terraces). The energetic repulsions presumably responsible for this behavior can be approximated by exclusions at separations of a small number of unit spacings. In the free-fermion context, the repulsive hard core L_c is increased from 0 to 3 or 1 in the cases of 1.3° and 2.5° misorientations, respectively. The modified distribution function is easily obtained by replacing the variable L by $L-L_c$ everywhere, including in $\langle L \rangle$. The resulting distributions describe the data quite well, except perhaps at the largest excluded spacing. So long as we restrict ourselves to infinite repulsions, we can maintain our temperature-independent formalism. For finite energetic interactions, most physically important mechanisms[27] have the same L^{-2} form as the entropic repulsion.[7]

Once the interactions have become sufficiently strong,[6] a Gaussian approximation provides a better description of the data. This "single-particle" form is the generalization, to a harmonic oscillator potential, of the particle in a box (Gruber-Mullins) discussed in Sec. III. In essence, for strong interactions it is more important to provide a good treatment of the single-step effects than to include multistep effects. For the physically important AL^{-2} interactions between fermions in 1D, Sutherland[28] finds the explicit form of $G_0(L)$ for two special values of A and shows more generally that one can evaluate the correlation functions in these cases in closed form by using Dyson's quaternion-determinant technique for the eigenvalues of random matrices.[29] (The third special case is just the free-fermion problem considered in this paper.) In the special case with repulsive interactions, $A=4k_BTz/(1+2z)\equiv A_R(T)$, where z is the Boltzmann weight of a single kink. The case with attractions requires $A=-A_R(T)/8$. To evaluate the scaled distribution for these interacting fermions, we cannot simply invoke the particle-hole symmetry used in Eq. (9). In prac-

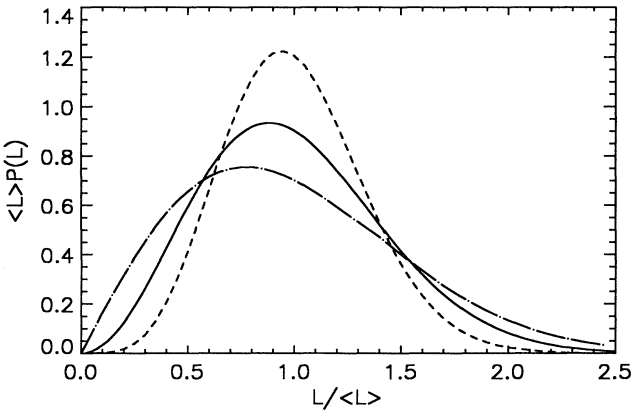

FIG. 5. Illustration of the alteration of the scaled "free-fermion" terrace-width distribution (solid curve) by energetic interactions proportional to L^{-2}, for the two other special cases for which the correlation functions can be evaluated in closed form (see text). The dashed curve shows the special case for repulsions; the scaled distribution is sharpened. The dot-dashed curve shows the special case for attractions.

tice, adequate numerical accuracy can be achieved by truncating the series of multiparticle correlation functions implicit in Eq. (8). Scaled terrace-width distribution functions for the three special cases are plotted in Fig. 5. The most striking qualitative difference in these curves is the leading behavior for small x: The scaled distributions rise as x^{β}, where $\beta=1$, 2, and 4 for the special cases of attractive, free, and repulsive fermions, respectively. Consistent with intuitive expectations, repulsions lead to a sharper $P(L)$, while attractions produce a broader distribution. Finally, when energetic interactions are important, temperature does influence $P(L)$.

ACKNOWLEDGMENTS

This work was supported partially (B.J.) by the Natural Sciences and Engineering Research Council of Canada and partially by the U.S. National Science Foundation under Grant No. DMR 88-02986. Some computing support was also provided by the University of Maryland Computer Science Center. We are grateful to Professor M. E. Fisher for helpful comments and for suggesting that we contact Professor H. Widom, whom we thank for sending a copy of Ref. 22 and for applying it for us to set down Eq. (30). We also thank Professor B. M. Baker for suggestions regarding Toeplitz matrices.

APPENDIX: ROLE OF MULTIPARTICLE INTERACTIONS

The role of multiparticle correlations can be crudely gauged by calculating the conditional probability $P(L)$ from a common probabilistic argument for random processes. Recall that the probability of having a step at L, if there is one at 0, is just $\langle L\rangle G_0(L)$ or, equivalently, $\langle L\rangle G(1,x)$. We denote this probability $P_0(L)$ to distinguish it from $P(L)$, for which there is *no* step between 0 and L. Now, if there are intermediate steps, suppose the first one is at L', which by definition has (conditional) probability $P(L')$. The probability of having steps at L' and at L (without regard to intermediate steps) is just $P_0(L-L')$. Summing over all the possibilities yields the identity

$$P_0(L)=P(L)+\sum_{L'=1}^{L-1}P(L')P_0(L-L')\ . \tag{A1}$$

This same equation is obtained in the Ornstein-Zernike theory of two-particle correlations in a liquid,[30] as well as other problems: (i) the probability of return of a lone random walker to his starting point [see Eq. (2.10) in Ref. 24] and (ii) the propagator of a particle scattering on equal s-wave δ function scatterers,[31] like an idealized pinball machine with identical pegs producing random scattering. All these situations share the common idea that correlations between two elements of the problem, positions, times, or particles, are sums of all possible pairs, with no three- or higher-body terms. For the random walker or the scattering particle, it means a total loss of memory at each step; for the liquid the direct correlations between two particles are independent of the positions of the other particles. The total correlation in the Ornstein-Zernike liquid is the sum of all possible trajectories linking two particles. In other words, the probability of each subsequent event is independent of previous events; not only multievent correlations are neglected, but so are two-event correlations. In the present context, the validity of Eq. (A1) would require that $P_0(L)$ be Q rather than $Q-(Q\pi^2L^2)^{-1}\sin^2\pi QL$; in that case, $P(L)$ would decay exponentially, following a Poisson distribution, amounting to the case of straight noninteracting steps illustrated in Fig. 2. Similarly, the Ornstein-Zernike theory of liquids neglects the oscillations in the direct correlations. Thus, when we include these effects below, we should not be surprised to find some unphysical effects from an approximation that seems sensible, but is somewhat inconsistent logically.

To solve for $P(L)$ using Eq. (A1), we start from $P(1)=P_0(1)$, take $P_0(L)$ from Eq. (5), and then iteratively generate each successive $P(L)$. The result is shown in Fig. 6. This approach, which would be exact if only pairwise correlations contributed, produces quite satisfactory results for values of x up to somewhat above the mean (viz., unity), indicating that multifermion correlations do not become really important until large values of x, when the core repulsions become important. To further elucidate this procedure, we take the expression for $P(2)$,

$$P(2)=P_0(2)-P_0^2(1)\ , \tag{A2}$$

substitute second-quantized operators as in Sec. II, and rearrange and cancel terms to find that Eq. (A2) is equivalent to the Kirkwood-like approximation[30]

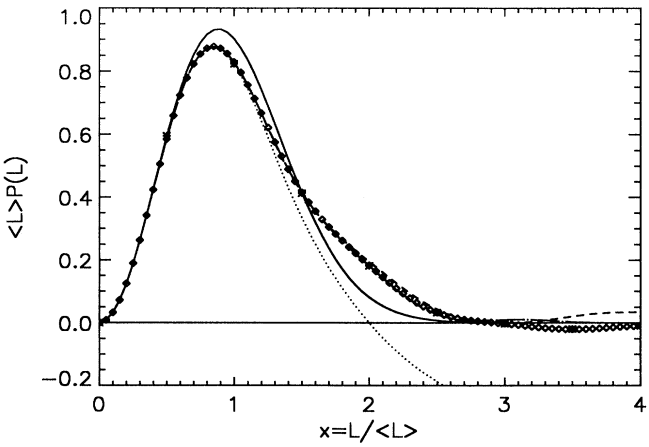

FIG. 6. Comparison of the limiting "universal" terrace-width distribution $f(x)$ (solid curve) with the scaled distribution obtained by straightforward iteration to solve Eq. (A1) for $\langle L\rangle=20$ (diamonds) and 2 (asterisks). The iteration result is obviously insensitive to the value of $\langle L\rangle$. Note that this procedure, based on common probabilistic arguments, works well for small x, but begins to deviate around the mean and becomes eventually negative for a range of large x. The dotted, dashed, and long-dash–dotted curves show the approximants of Eqs. (A7), (A8), and (A9) respectively. The approximant of Eq. (A6) is just the curve labeled 1 in Fig. 4.

$$\langle 0|a_0^\dagger a_0 a_1^\dagger a_1 a_2^\dagger a_2|0\rangle \approx \langle 0|a_0^\dagger a_0 a_1^\dagger a_1|0\rangle \langle 0|a_1^\dagger a_1 a_2^\dagger a_2|0\rangle / \langle 0|a_1^\dagger a_1|0\rangle \ , \tag{A3}$$

where $\langle 0|a_1^\dagger a_1|0\rangle$ is just Q. The result of the iteration as a pairwise decomposition can perhaps best be described in terms of a prescription for the sequence of $P(L)$'s: Write down the sequence of sites 0,1,2,3, . . . , L. Construct all possible ways to hop with ever-increasing site from 0 to L by means of some (sub)set of the intermediate sites. Associate each hop with the P_0 for the difference of site indices and each path from 0 to L with the product of these P_0's, i.e., a pairwise decomposition. Then $P(L)$ is the sum of these various products of P_0's, with the proviso that terms with an even number of P_0's have a minus sign rather than a plus. (If instead we solved for P_0 in terms of P, we would not need the minus-sign proviso, and the result is somewhat more transparent.) With this prescription, the next two interactions are

$$P(3)=P_0(3)-2P_0(1)P_0(2)+P_0^2(1) \ , \tag{A4}$$

$$P(4)=P_0(4)-[P_0^2(2)+2P_0(1)P_0(3)]+3P_0^2(1)P_0(2)-P_0^4(1) \ . \tag{A5}$$

To appreciate the behavior of these pairwise iterations and their limit, we can produce a sequence of analytic approximants, as in the preceding section:

$$\frac{G(1,x)}{Q^2} \doteq 1-\frac{\sin^2\pi x}{\pi^2 x^2} \equiv H(x) \ , \tag{A6}$$

$$\frac{G(2,x)}{Q^2} \doteq H(x)-\frac{x}{2}H^2\left[\frac{x}{2}\right] \ , \tag{A7}$$

$$\frac{G(3,x)}{Q^2} \doteq H(x)-2\frac{x}{3}H\left[\frac{x}{3}\right]H\left[\frac{2x}{3}\right]+\left[\frac{x}{3}\right]^2 H^3\left[\frac{x}{3}\right] \ , \tag{A8}$$

$$\frac{G(4,x)}{Q^2} \doteq H(x)-\left[\frac{x}{4}\right]\left[H^2\left[\frac{x}{2}\right]+2H\left[\frac{3x}{4}\right]H\left[\frac{x}{4}\right]\right]+3\left[\frac{x}{4}\right]^2 H^2\left[\frac{x}{4}\right]H\left[\frac{x}{2}\right]-\left[\frac{x}{4}\right]^3 H^4\left[\frac{x}{4}\right] \ . \tag{A9}$$

These approximants are plotted in Fig. 6. They have the same behavior near $x=0$ and n as the previous ones [Eqs. (16), (20), and (23)], but the convergence, as rapid as for the previous approximants, is to the limiting solution of Eq. (A1) instead of the predictions of the free-fermion model. The neglect of multiparticle correlations evidently leads to oscillations about the free-fermion result, presumably associated with the sign of the contribution of different channels: Near the peak, the pairwise iterative result is too small, while in the following tail it is too large (and has a curious shoulder). For $x \geq 3$, $f(x)$ is negligible for practical purposes, but we have extended the plot to show the small negative dip that occurs. This highly unphysical result shows that the pair approximation becomes particularly dangerous above thrice the interparticle spacing and is a manifestation of the inconsistency of this approach, showing that in this approximation $P(L)$ is not a well-defined probability.

---

*Permanent address: Ottawa Carleton Institute of Physics, University of Ottawa Campus, Ottawa, Ontario, Canada K1N 6N5. Electronic address: BJOSJ@UOTTAWA.BITNET.

†Electronic address: TEDEINST@UMDD.UMD.EDU.

‡Electronic address: BARTELT@SURFACE.UMD.EDU.

[1]C. Herring, Phys. Rev. **82**, 87 (1951).

[2]M. Wortis, in *Chemistry and Physics of Solid Surfaces,* edited by R. Vanselow and R. Howe (Springer-Verlag, Berlin, 1988), Vol. 7, p. 367.

[3]R. J. Phaneuf and E. D. Williams, Phys. Rev. Lett. **58**, 2563 (1987); Phys. Rev. B **41**, 2991 (1990); R. J. Phaneuf, E. D. Williams, and N. C. Bartelt, *ibid.* **38**, 1984 (1988); B. S. Swartzentruber, Y.-W. Mo, M. B. Webb, and M. G. Lagally, J. Vac. Sci. Technol. A **7**, 2901 (1989); J. E. Griffith and G. P. Kochanski, Crit. Rev. Solid State Mater. Sci. **16**, 255 (1990).

[4]G. S. Bales and A. Zangwill, Phys. Rev. B **41**, 5500 (1990).

[5]M. E. Fisher and D. S. Fisher, Phys. Rev. B **25**, 3192 (1982); M. E. Fisher, J. Chem. Soc. Faraday Trans. 2 **82**, 1569 (1986).

[6]N. C. Bartelt, T. L. Einstein, and Ellen D. Williams, Surf. Sci. Lett. **240**, L591 (1990).

[7]C. Jayaprakash, C. Rottman, and W. F. Saam, Phys. Rev. B **30**, 6549 (1984).

[8]A recent review discussing the TSK and solid-on-solid models is H. van Beijeren and I. Nolden, in *Structure and Dynamics of Surfaces II,* edited by W. Schommers and P. von Blanckenhagen (Springer-Verlag, Berlin, 1987), p. 259.

[9]T. L. Einstein, N. C. Bartelt, J. L. Goldberg, X.-S. Wang, E. D. Williams, and B. Joós, in *The Structure of Surfaces III,* edited by S. Y. Tong, M. A. Van Hove, X. Xide and K. Takayanagi (Springer-Verlag, Berlin, 1991).

[10]B. S. Swartzentruber, Y.-W. Mo, R. Kariotis, M. G. Lagally, and M. B. Webb, Phys. Rev. Lett. **65**, 1913 (1990).

[11]N. C. Bartelt, T. L. Einstein, and E. D. Williams, Surf. Sci. **244**, 149 (1991).

[12]X.-S. Wang, J. L. Goldberg, N. C. Bartelt, T. L. Einstein, and Ellen D. Williams, Phys. Rev. Lett. **65**, 2430 (1990).

[13]Y.-N. Yang, B. M. Trafas, R. L. Siefert, and J. H. Weaver, Bull. Am. Phys. Soc. **36**, 910 (1991).

[14]D. A. Huse and M. E. Fisher, Phys. Rev. B **29**, 239 (1984).

[15]M. den Nijs, in *Phase Transitions and Critical Phenomena,* edited by C. Domb and J. L. Lebowitz (Academic, Orlando,

FL, 1988), Vol. 12, p. 219.
[16]J. B. Kogut, Rev. Mod. Phys. **51**, 659 (1979), in particular, p. 668.
[17]P. G. de Gennes, J. Chem. Phys. **48**, 2257 (1968).
[18]G. Baym, *Lectures on Quantum Mechanics* (Benjamin, Reading, MA, 1969), Chap. 19, p. 427.
[19]B. M. McCoy and T. T. Wu, *The Two-Dimensional Ising Model* (Harvard University Press, Cambridge, MA, 1973).
[20]U. Grenander and G. Szegö, *Toeplitz Forms and Their Applications* (University of California Press, Berkeley, 1958).
[21]E. E. Gruber and W. W. Mullins, J. Phys. Chem. Solids **28**, 875 (1967).
[22]H. Widom, Indiana Univ. Math. J. **21**, 277 (1971).
[23]H. Widom (private communication).
[24]M. E. Fisher, J. Stat. Phys. **34**, 667 (1984).
[25]L. V. Mikheev and V. L. Pokrovsky, J. Phys. (Paris) **1**, (1991).
[26]N. C. Bartelt and T. L. Einstein (unpublished).
[27]O. L. Alerhand, D. Vanderbilt, R. D. Meade, and J. D. Joannopoulos, Phys. Rev. Lett. **61**, 1973 (1988), and references therein.
[28]Bill Sutherland, J. Math. Phys. **12**, 246, 251 (1971); Phys. Rev. A **4**, 2019 (1971).
[29]F. J. Dyson, Commun. Math. Phys. **19**, 235 (1970), in particular, theorem 1.
[30]R. O. Watts and I. J. McGee, *Liquid State Chemical Physics* (Wiley, New York, 1976), Sec. 3.8; J. P. Hansen and I. R. McDonald, *Theory of Simple Liquids,* 2nd ed. (Academic, London, 1986), Sec. 5.2.
[31]R. Mattuck, *A Guide to Feynman Diagrams in the Many-Body Problem,* 2nd ed. (McGraw-Hill, New York, 1976).